Z. Phys. C - Particles and Fields 26, 353-358 (1984)

Zeitschrift für Physik C Particles and Fields
© Springer-Verlag 1984

A Measurement of the Q^2 and W Dependence of the $\gamma\gamma$ Total Cross Section for Hadron Production

PLUTO Collaboration

Ch. Berger, A. Deuter, H. Genzel, W. Lackas, J. Pielorz[a], F. Raupach[b], W. Wagner[c]
I. Phys. Institut der RWTH Aachen[d], D-5100 Aachen, Federal Republic of Germany

A. Klovning, E. Lillestöl
University of Bergen[e], N-5014 Bergen, Norway

J. Bürger, L. Criegee, F. Ferrarotto[f], G. Franke, M. Gaspero[f], Ch. Gerke[g], G. Knies, B. Lewendel, J. Meyer, U. Michelsen, K.H. Pape, B. Stella[f], U. Timm, G.G. Winter, M. Zachara[h], W. Zimmermann
Deutsches Elektronen-Synchrotron DESY, D-2000 Hamburg, Federal Republic of Germany

P.J. Bussey, S.L. Cartwright[i], J.B. Dainton, B.T. King, C. Raine, J.M. Scarr, I.O. Skillicorn, K.M. Smith, J.C. Thomson
University of Glasgow[j], Glasgow G 12 8QQ, UK

O. Achterberg[k], V. Blobel, D. Burkart, K. Diehlmann, M. Feindt, H. Kapitza, B. Koppitz, M. Krüger, M. Poppe, H. Spitzer, R. van Staa
II. Institut für Experimentalphysik der Universität, D-2000 Hamburg[d], Federal Republic of Germany

C.Y. Chang, R.G. Glasser, R.G. Kellogg, S.J. Maxfield, R.O. Polvado[m], B. Sechi-Zorn, J.A. Skard, A. Skuja, A.J. Tylka, G.E. Welch, G.T. Zorn
University of Maryland[n], USA

F. Almeida[o], A. Bäcker, F. Barreiro, S. Brandt, K. Derikum[p], C. Grupen, H.J. Meyer, H. Müller, B. Neumann, M. Rost, K. Stupperich, G. Zech
Universität-Gesamthochschule Siegen[d], Federal Republic of Germany

G. Alexander, G. Bella, Y. Gnat, J. Grunhaus
University of Tel-Aviv[q], Israel

H. Junge, K. Kraski, C. Maxeiner, H. Maxeiner, H. Meyer, D. Schmidt
Universität-Gesamthochschule Wuppertal[d], D-5600 Wuppertal, Federal Republic of Germany

Received 10 September 1984

[a] Deceased
[b] Now at Université de Paris Sud, F-91405 Orsay, France
[c] Now at University of California at Davis, Ca., USA
[d] Supported by the BMFT, Federal Republic of Germany
[e] Partially supported by Norwegian Council for Science and Humanities
[f] Rome University, partially supported by I.N.F.N., Sezione di Roma, Italy
[g] Now at CERN, CH-1211 Geneva 23, Switzerland
[h] Institute of Nuclear Physics, P-30055 Cracow, Poland
[i] Now at Rutherford Appleton Laboratory, Chilton, UK
[j] Supported by the U.K. Science and Engineering Research Council
[k] Now at Texaco Europe Computer Information Systems, Hamburg, FRG
[l] Now at Universität Karlsruhe, D-7500 Karlsruhe, FRG
[m] Now at Northeastern University, Boston, Mass., USA
[n] Partially supported by the Department of Energy, USA
[o] On leave of absence from Inst. de Fisica, Universidad Federal do Rio de Janeiro, Brasil
[p] Now at BESSY, D-1000 Berlin, Germany
[q] Partially supported by the Israeli Academy of Sciences and Humanities - Basic Research Foundation

Abstract. A measurement of the $\gamma\gamma$ total cross section, $\sigma_{\gamma\gamma}(Q^2, W)$, is presented for the Q^2 range 0.1 to 100 GeV^2, and for the mass W of the hadronic final state between 1.5 and 10 GeV. The dependence of $\sigma_{\gamma\gamma}$ on both Q^2 and W is measured. The results are compared with theoretical predictions. It is found that the data are well described by a sum of quark-parton model and vector dominance contributions.

Hadron production in two-photon ($\gamma\gamma$) collisions may take place through the interaction of the hadronic components of one or both photons, or through the point-like coupling of the interacting photons to quark-antiquark ($q\bar{q}$) pairs (Fig. 1). According to VDM the hadronic photon component is expected to be large at low Q^2 and to be suppressed by vector meson propagators at high Q^2. The point-like component, as calculated in QPM or QCD, has a weak Q^2 dependence and is thus expected to become relatively more important at large Q^2. In addition, the interaction cross sections of the two components are expected to have different dependences on W, the hadronic invariant mass.

It is therefore interesting to investigate both the Q^2 and W dependence of the $\gamma\gamma$ total hadronic cross section, $\sigma_{\gamma\gamma}$, over a large range. This paper presents a study of the process $e^+e^- \to e^+e^- +$hadrons, using the detector PLUTO at PETRA, for the Q^2 range 0.1 to 100 GeV^2 and W between 1.5 and 10 GeV. Our results are corrected for experimental acceptance and measurement errors and can thus be compared directly with theory.

If one of the scattered electrons is detected (tagged) by suitably placed electromagnetic shower counters, the Q^2 (absolute value of the invariant mass squared) of the associated virtual photon can be determined from its scattering angle, ϑ_1 and energy, E_1. If, additionally, a veto is applied to ensure that the other scattered electron remains at small angles ($\vartheta_2 < \vartheta_{2\,\max}$), it is possible to express the cross section for the observed process as:

$$d\sigma(e^+e^- \to e^+e^- + X) = \frac{\alpha E_1(1+(1-y)^2)}{2\pi^2 Q^2 y}\{\sigma_{TT}+\varepsilon\sigma_{TL}\}N(z,\vartheta_{2\,\max})dz dE_1 d\Omega \quad (1)$$

where σ_{TT} and σ_{TL} are the $\gamma\gamma$ cross sections for transversely and longitudinally polarised probe photons respectively and ε represents the ratio of their fluxes. $N(z, \vartheta_{2\,\max})$ describes the flux of quasi-real target photons [1, 2] of fractional energy z; y is determined from the tagged electron:

$$y = 1 - (E_1/E_{\text{beam}})\cos^2(\vartheta_1/2). \quad (2)$$

Hereafter we refer to the quantity $(\sigma_{TT}+\sigma_{TL})$ as $\sigma_{\gamma\gamma}$.

From the above expression it may be noticed that the data measure the quantity $\sigma_{TT}+\varepsilon\sigma_{TL}$. However, within the tag energy and angle constraints imposed on the data, y is small so that $\varepsilon \sim 1$ and we measure $\sigma_{\gamma\gamma}$. A correction for the deviation of ε from unity is, in principle, necessary for our high Q^2 data ($Q^2 > 20$ GeV^2), where $\langle\varepsilon\rangle = 0.91$. The size of this correction depends on the relative importance of σ_{TT} and σ_{TL}. If these two cross sections are calculated [2] from $\gamma\gamma \to q\bar{q}$, $\sigma_{TT}+\varepsilon\sigma_{TL}$ is 2% lower than $\sigma_{\gamma\gamma}$ for $Q^2 > 20$ GeV^2. At lower Q^2 the correction is even smaller. Since this correction is model dependent (but small within the context of the QPM model) we present the data uncorrected.

The data were taken with the PLUTO detector at the e^+e^- storage ring PETRA at a beam energy of 17.3 GeV. Since the publication of the first results on the total $\gamma\gamma$ cross section [3], the PLUTO detector has been upgraded to improve the angular coverage in the forward direction. This allows a more complete reconstruction of the events and con-

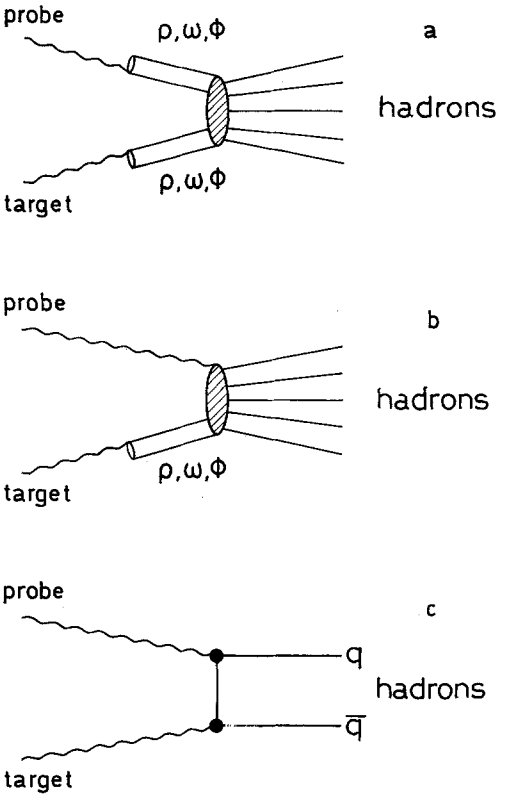

Fig. 1a–c. Schematic representation of $\gamma\gamma$ coupling to hadrons via **a** hadronic behaviour of both photons; **b** hadronic behaviour of the target photon only; and **c** point-like $q\bar{q}$ coupling

Table 1. Parameters of the PLUTO tagging devices

	Angular Range	$\sigma_E/\sqrt{E}$ (E in GeV)	Q^2 Range (GeV^2)	σ_{Q^2}/Q^2
SAT	30- 55 mrad	16.5%	0.1- 1	10%
LAT	90-260 mrad	25%	1 - 20	10%
EC	330-680 mrad	28%	15 -130	10%

sequently, less dependence of the results on Monte-Carlo simulation of the experiment.

Details of the PLUTO detector have been given in previous publications [4]. Here we outline the detection of the tagged electrons, which are identified as single isolated showers in either the Small Angle Tagger (SAT), Large Angle Tagger (LAT) or the Endcap (EC). Each of these detectors consists of lead scintillator shower counters located behind track chambers which give good spatial resolution and distinguish between photons and electrons. The polar angular ranges, Q^2 ranges and resolutions and energy resolutions of these devices are given in Table 1.

The data presented here were taken using three separate triggers:

1. A SAT tag ($E_1 > 6$ GeV)+one short track in the central detector.
2. A LAT tag ($E_1 > 4$ GeV).
3. A EC tag ($E_1 > 3$ GeV).

No track was required for the LAT and EC triggers to be satisfied.

The following event selection criteria were defined to optimize the acceptance and minimize the background contamination:

a) Tagging requirement: irrespective of the tagging device in which it was found, the tagged electron was required to have energy $E_1 > 8$ GeV. This condition removed those events for which y was large, keeping the value of ε close to unity.

b) Anti-tag criterion: to keep the invariant mass squared, $-P^2$, of the target photon close to zero, all events were rejected in which a shower with energy > 4 GeV was found in the LAT or SAT opposite to the tag.

c) Multiplicity requirement: to be accepted as a multihadronic final state, events had to have either $\geqq 3$ charged tracks or two charged tracks plus neutral showers. To suppress the background from QED processes, 2 and 3 track events with a clearly identified electron in the final state were removed.

d) Range of final state invariant mass: the invariant mass, W_{vis}, of the observed final state hadrons was limited to $1.2 < W_{\text{vis}} < 10$ GeV to reduce contamination from radiative annihilation events and to avoid the low W region for which the acceptance is small and is difficult to estimate.

e) Beam gas rejection: to reduce the contamination from beam-gas events the z-coordinate of the vertex was required to be within ± 40 mm from the nominal interaction point, where z is the direction along the beam line.

f) For EC tagged events, the missing electron, reconstructed using momentum conservation, was required to have a momentum of at least 6 GeV along the beam axis opposite to the tag. This condition was necessary to suppress the background from annihilation processes in the EC data.

The above selection criteria resulted in 2929, 1587 and 105 events tagged in the SAT, LAT and EC angular ranges respectively. The residual background from beam-gas events was determined from the side-bands of the event vertex distribution. All remaining contributions from e^+e^- annihilation, $\gamma\gamma$ QED processes and inelastic Compton scattering have been estimated using Monte-Carlo techniques and subtracted from the data. For the SAT the most important background was due to beam-gas processes (4%). At larger angles the most important background was $\gamma\gamma \to \tau^+\tau^-$, with a contribution ranging from 1.5% in the SAT data, to 5% in the LAT and 10% in the EC region.

Due to particle losses and finite resolution the observed final state invariant mass, W_{vis}, is in general different from the true value, W. To extract the cross section, $\sigma_{\gamma\gamma}(Q^2, W)$, from the selected data, Monte-Carlo events were generated according to (1) with the quantity $\sigma_{\gamma\gamma}$ set equal to a constant. This procedure simulates the photon fluxes and detector acceptance. After all selection criteria were applied, these events, together with the data, were passed through an unfolding procedure [5]. The relation between the observed event distribution $N(W_{\text{vis}})$ and the cross section, $\sigma_{\gamma\gamma}(W)$, can be written:

$$N(W_{\text{vis}}) = \int A(W_{\text{vis}}, W)\,\sigma_{\gamma\gamma}(W)\,dW. \tag{3}$$

The function $A(W_{\text{vis}}, W)$, determined from the Monte-Carlo events, is proportional to the probability of observing an event at a given W_{vis} for a given true W and thus describes the effects of limited detector acceptance and resolution. The unfolding procedure iteratively adjusts $\sigma_{\gamma\gamma}(W)$ to produce the best description of the observed distribution. There are two important complications to this procedure. Firstly, the relation between true and visible quantities depends on the fragmentation model assumed for the hadronisation of the W system. Secondly, the data are not all at the same Q^2.

We have tried different models for the fragmenta-

tion of the $\gamma\gamma$ system. Most models can be excluded by comparing the visible distributions of the data (e.g. multiplicity, p_{T2}) with the corresponding simulated distributions, after weighting the Monte Carlo events by the unfolded cross section. The fragmentation models found to fit the data best for each of the Q^2 ranges are described in detail in the publications dealing with the SAT, LAT and EC samples separately [6–8]. It was found that W dependent mixtures of isotropic and limited p_T (to the $\gamma\gamma$ axis) phase space models, together with KNO [9] multiplicity distributions, were appropriate at low and intermediate Q^2. For high Q^2 (EC data) at high W, the W system is first transformed into a $q\bar{q}$ pair with angular distribution to the $\gamma\gamma$ axis given by QED. Subsequently the quarks were fragmented according to the standard Feynman-Field prescription [10].

To overcome the problem that each of the data samples actually consists of a range of Q^2 values, the data were interpolated to fixed Q^2 values at the average Q^2 of the sample under consideration. The omission of this interpolation procedure changes the results by less than 10%.

The dependence of the cross section on Q^2 and W, extracted using the methods described above, is presented in Table 2, together with the statistical and systematic error of each point. We have investigated the systematic errors inherent in the cross section determinations due to fragmentation uncertainties and due to the criteria used to select the data. To this end we have varied the fragmentation models used in the Monte-Carlo simulation within the constraint that the observed data distributions must be adequately reproduced. The systematic error of $\sigma_{\gamma\gamma}(Q^2)$, averaged over the W interval 3 to 10 GeV, due to the uncertainty in the fragmentation, is 5 to 10% which is comparable to the statistical errors. However, within individual W intervals the systematic error is greater, the lowest and highest W points being most sensitive to variation of fragmentation parameters. We estimate the systematic error on these points to be 25% and to be 15% for the remainder of the W bins.

We have also studied the dependence of our results on the event selection criteria. The most noticeable effect came from inclusion of events with fewer than four charged tracks. Removing those events with three or less charged tracks caused the unfolded cross sections to change by less than the effects of varying the hadronisation models, thus giving confidence that the background from QED processes was small and correctly subtracted.

The Q^2 dependence of the cross section, averaged over the W range $3 < W < 10$ GeV, is shown in Fig. 2 and given in Table 2. Also shown, in Fig. 2a, is the

Table 2. The measured photon-photon cross sections $\sigma_{\gamma\gamma}(Q^2, W)$ together with the statistical and systematic errors

$\sigma_{\gamma\gamma}(Q^2, W)$ (nb)

Q^2(GeV^2)	W Range (GeV)					
	1.5–2	2–3	3–4	4–6	6–8	8–10
0.44	309 ±21 ±77	241 ±11 ±24	182 ±14 ±27	144 ±17 ±22	107 ±24 ±21	125 ±39 ±31
5.4	52.5 ±9.5 ±13	57.9 ±3.7 ±9	57.3 ±3.5 ±9	50.3 ±3.5 ±7	40.1 ±4.9 ±6	42.6 ±8.2 ±11
	W Range (GeV)					
	1.7–3		3–6		6–10	
45	13.6 ± 6.3 ± 3.4		16.6 ± 2.9 ± 2.5		13.5 ± 2.9 ± 3.4	

$$\langle\sigma_{\gamma\gamma}(Q^2)\rangle = \int_3^{10} \sigma_{\gamma\gamma}(Q^2, W)dW \Big/ \int_3^{10} dW$$

Q^2 (GeV^2)	$\langle\sigma_{\gamma\gamma}(Q^2)\rangle$ (nb)
0.30	163 ±16 ±16
0.57	116 ±12 ±12
2.4	70.5 ± 6.2 ± 3.5
4.3	57.8 ± 3.7 ± 3.0
9.2	31.6 ± 2.6 ± 1.6
30.0	19.0 ± 3.3 ± 1.0
65.0	11.1 ± 2.4 ± 0.6

prediction of the point-like contribution. It is calculated using the QED Born amplitude given by [2] but assuming quark charges, masses and colour factors for the production of u, d, s and c quark pairs (QPM). For u and d quarks masses of 300 MeV were used, whilst for s and c quarks the values 500 MeV and 1.6 GeV were taken respectively. As can be seen, at high Q^2 the QPM prediction approaches the data, while at low Q^2 it is significantly below. This excess data may be accounted for by the hadronic component of the photon. We find that by adding a contribution of the form $A \cdot F_{\mathrm{GVDM}}(Q^2)$, where F_{GVDM} is the Q^2 dependence of the Generalised Vector Dominance Model (GVDM) [11], the data are well described over the full Q^2 range with $A = (232 \pm 15)$ nb. It is obvious that a GVDM term alone cannot describe the Q^2 dependence of the data. We note in passing that such an addition of QPM and VDM may result in double counting [12]. Nevertheless, this procedure describes the data over its entire Q^2 range.

The data are compared with three other models for the Q^2 development of the total $\gamma\gamma$ cross section

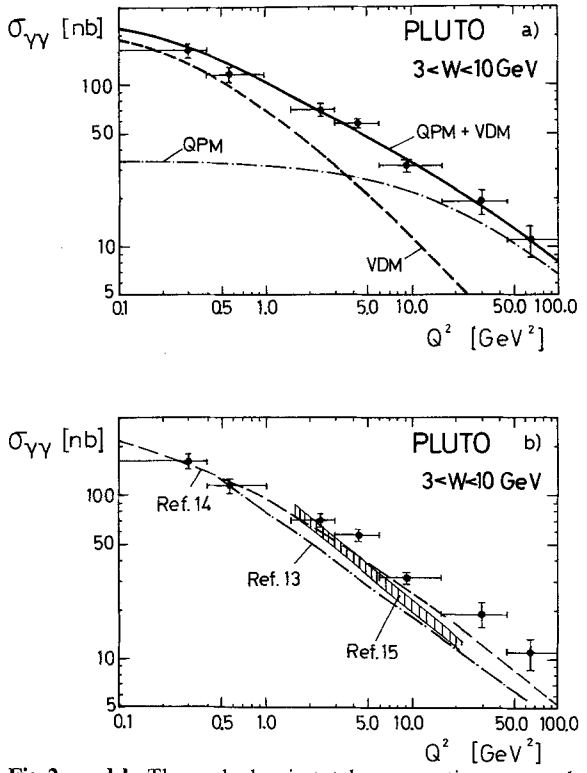

Fig. 2a and b. The $\gamma\gamma$ hadronic total cross section averaged over the W range $3<W<10$ GeV, plotted as a function of Q^2. In **a** the data are compared with a VDM estimate consisting of a GVDM form factor normalised to 232 nb at zero Q^2, the QPM estimate discussed in the text, and the sum of these two estimates. Only statistical errors are shown. In **b** the same data are compared with the models proposed in [13–15]

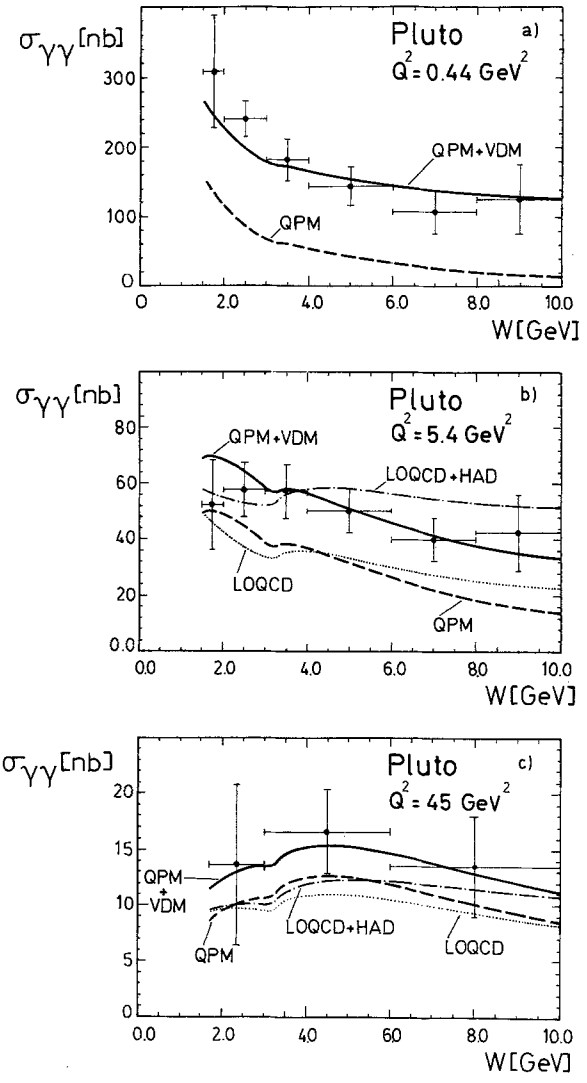

Fig. 3a–c. The $\gamma\gamma$ hadronic total cross section as a function of W for three values of Q^2. **a** $Q^2=0.44\,\mathrm{GeV}^2$; dashed line QPM, solid line QPM plus a VDM term of the form $232\,\mathrm{nb}\cdot F_{\mathrm{GVDM}}(Q^2)$. **b** $Q^2=5.4\,\mathrm{GeV}^2$; dashed and solid lines are QPM and QPM+VDM respectively; also shown are the LOQCD and the sum of LO-QCD and hadronic contribution (see text). **c** $Q^2=45\,\mathrm{GeV}^2$; curves as in **b** evaluated at $Q^2=45\,\mathrm{GeV}^2$. The errors shown correspond to the statistical and systematic errors added in quadrature

in Fig. 2b. Two of these models [13, 14] assume that photon-hadron coupling occurs via an infinite series of vector mesons, whilst the other model [15] is based upon a factorisation approach for $\sigma_{\gamma\gamma}$, using results from γp, ep and pp data. Like the GVDM, these models predict a steeper Q^2 dependence than seen in the data, the nearest approach is that of [14].

The W dependence of $\sigma_{\gamma\gamma}$ is presented in Fig. 3a–c for three values of Q^2. For Fig. 3a, the SAT data (Q^2 range 0.1 to $1\,\mathrm{GeV}^2$) are interpolated to $Q^2=0.44\,\mathrm{GeV}^2$. In Fig. 3b, the LAT data (Q^2 range 1.5 to $16\,\mathrm{GeV}^2$) are used to determine $\sigma_{\gamma\gamma}(W)$ at $Q^2=5.4\,\mathrm{GeV}^2$. The EC data (Q^2 range 16 to $100\,\mathrm{GeV}^2$) are presented in Fig. 3c at $Q^2=45\,\mathrm{GeV}^2$. Figure 3 shows that the measured cross section does not factorise in W and Q^2. Each plot is compared with the QPM prediction plus a W independent term, the value of which has been obtained from the fit to Fig. 2a. This parameterisation is seen to describe the W dependence of the cross section at all Q^2. With this parameterisation no requirement for a $1/W$ hadronic component is apparent in our data.

Next we take a QCD prediction for the point-like contribution. The leading order QCD prediction [16] for the photon structure function, $F_2(x,Q^2)$, has been converted to the cross section $\sigma_{\gamma\gamma}(Q^2,W)=F_2(x,Q^2)\,4\pi^2\alpha/Q^2$, where $x=Q^2/(Q^2+W^2)$. We show in Fig. 3, for the LAT and EC samples, this leading order QCD prediction added to a charm contribution calculated using QPM as described above. We refer to this sum as LOQCD. The hadronic component is parameterised [17] as $F_2(x)=0.2\alpha(1-x)$. This structure function treatment is inappropriate at low Q^2 and we therefore omit this analysis for the SAT data. It is clear that, with $\Lambda\sim 200$ MeV, LOQCD is closely equal to the QPM.

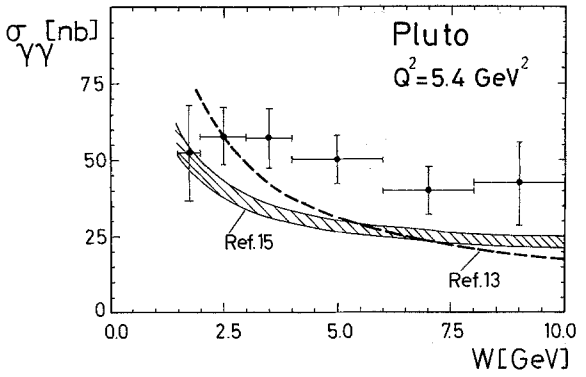

Fig. 4. The cross section $\sigma_{\gamma\gamma}(W, Q^2 = 5.4\,\mathrm{GeV}^2)$ is compared with the factorisation model of [15] and with the model of [13]. The errors shown correspond to the statistical and systematic errors added in quadrature

The sum of LOQCD and the hadronic component describes the general trend of the data as a function of W.

We also show, in Fig. 4, $\sigma_{\gamma\gamma}(W)$ for the LAT data at $Q^2 = 5.4\,\mathrm{GeV}^2$ compared to the factorisation model of reference 15 and with the model of [13]. These models fail to describe the data.

In conclusion, we have measured the $\gamma\gamma$ hadronic cross section as a function of W at $Q^2 = 0.44$, 5.4, and 45 GeV^2. In addition, we have measured the Q^2 dependence of $\sigma_{\gamma\gamma}$ averaged over the W interval $3 < W < 10\,\mathrm{GeV}$. We find that a sum of two terms, namely a QPM term representing the point-like $\gamma\gamma$ interaction and a VDM term of the form $(232 \pm 15)\,\mathrm{nb} \cdot F_{\mathrm{GVDM}}(Q^2)$ representing the hadronic $\gamma\gamma$ interaction, describes well the W and Q^2 dependence of $\sigma_{\gamma\gamma}$. It is interesting to note that this parameterisation also fits the observed jet production properties of our data [18]. Models based solely upon vector meson dominance or factorisation [13, 15] do not by themselves reproduce the data over the whole W and Q^2 region. However, a fair agreement with the data can be obtained by adding a QPM term to these models.

Acknowledgements. We wish to thank the members of the DESY directorate for the hospitality extended to the university groups. We are indebted to the PETRA machine group and the DESY computer centre for their excellent performance during the experiment. We gratefully acknowledge the efforts of all engineers and technicians who have participated in the construction and maintenance of the apparatus.

References

1. C. Carimalo, P. Kessler, J. Parisi: Phys. Rev. **D 21**, 669 (1980)
2. V.M. Budnev at al.: Phys. Rep. **15 C**, 181 (1975)
3. PLUTO Collab. Ch. Berger et al.: Phys. Lett. **99 B**, 287 (1981)
4. PLUTO Collab. Ch. Berger et al.: Z. Phys. C - Particles and Fields **26**, 199 (1984); Steve Maxfield Ph.D. thesis. (University of Maryland)
5. V. Blobel: Proceedings of the 1984 CERN school of computing. Aiguablava, September 1984. To be published
6. Measurement of the total photon-photon cross section for the production of hadrons at small Q^2, PLUTO Collaboration. To be published
7. PLUTO Collab., Ch. Berger et al.: Phys. Lett. **142 B**, 111 (1984)
8. Measurement and QCD analysis of the photon structure function $F_2(x, Q^2)$ PLUTO Collaboration. To be published.
9. Z. Koba, H.B. Nielson, P. Oleson: Nucl. Phys. **B 40**, 317 (1972)
10. R.P. Feynman, R.D. Field: Nucl. Phys. **B 136**, 1 (1978)
11. J.J. Sakurai, D. Schildknecht: Phys. Lett. **41 B**, 121 (1972); I.F. Ginzburg, V.G. Serbo: Phys. Lett. **109 B**, 231 (1982)
12. M. Glück, K. Grassi, E. Reya: University of Dortmund preprint DO-TH 83/23 (1983)
13. U. Maor, E. Gotsman: Phys. Rev. **D 28**, 2149 (1983); U. Maor: private communication
14. E. Etim, E. Massó, L. Schülke: Z. Phys. C - Particles and Fields **18**, 361 (1983)
15. G. Alexander, U. Maor, C. Milstene: Phys. Lett. **131 B**, 224 (1983)
16. E. Witten: Nucl. Phys. **B 120**, 189 (1977)
17. C. Peterson, T.F. Walsh, P.M. Zerwas: Nucl. Phys. **B 174**, 424 (1980); W. Wagner: RWTH Aachen preprint PITHA 83/03 (1983)
18. PLUTO Collab. Ch. Berger et al.: Z. Phys. C - Particles and Fields **26**, 191 (1984)